Article

Polycationic β-Cyclodextrin "Click Clusters": Monodisperse and Versatile Scaffolds for Nucleic Acid Delivery

Sathya Srinivasachari, Katye M. Fichter, and Theresa M. Reineke

J. Am. Chem. Soc., **2008**, 130 (14), 4618-4627 • DOI: 10.1021/ja074597v

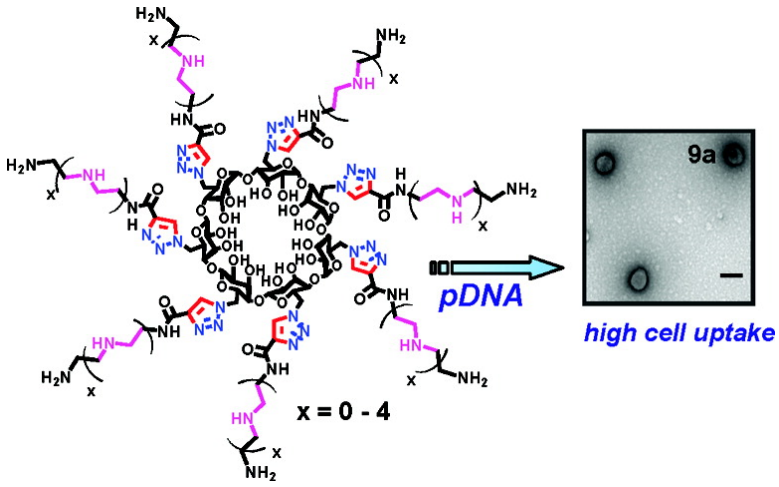

More About This Article

Additional resources and features associated with this article are available within the HTML version:

- Supporting Information
- Links to the 3 articles that cite this article, as of the time of this article download
- Access to high resolution figures
- Links to articles and content related to this article
- Copyright permission to reproduce figures and/or text from this article

View the Full Text HTML

J|A|C|S
ARTICLES
Published on Web 03/14/2008

Polycationic β-Cyclodextrin "Click Clusters": Monodisperse and Versatile Scaffolds for Nucleic Acid Delivery

Sathya Srinivasachari, Katye M. Fichter, and Theresa M. Reineke*

Department of Chemistry, University of Cincinnati, Cincinnati, Ohio 45221-0172

Received June 22, 2007; E-mail: Theresa.Reineke@uc.edu

Abstract: Herein, a novel series of multivalent polycationic β-cyclodextrin "click clusters" with discrete molecular weight have been synthesized, characterized, and examined as therapeutic pDNA carriers. The materials were creatively designed based on a β-cyclodextrin core to impart a biocompatible multivalent architecture and oligoethyleneamine arms to facilitate pDNA binding, encapsulation, and cellular uptake. An acetylated-per-azido-β-cyclodextrin (**4**) was reacted with series of alkyne dendrons (**7a**−**e**) (containing one to five ethyleneamine units) using copper-catalyzed 1,3-dipolar cycloaddition, to form a series of click clusters (**9a**−**e**) bearing 1,2,3-triazole linkers. Gel electrophoresis experiments, dynamic light scattering, and transmission electron microscopy revealed that the macromolecules bind and compact pDNA into spherical nanoparticles in the size range of 80−130 nm. The polycations protect pDNA against nuclease degradation, where structures **9c**, **9d**, and **9e** did not allow pDNA degradation in the presence of serum for up to 48 h. The cellular uptake profiles were evaluated in Opti-MEM and demonstrate that all the click clusters efficiently deliver Cy5-labeled pDNA into HeLa and H9c2 (2−1) cells, and compounds **9d** and **9e** yielded efficacy similar to that of the positive controls, Jet-PEI and Superfect. Furthermore, the luciferase gene delivery experiments revealed that the level of reporter gene expression increased with an increase in oligoethyleneamine number within the cluster arms. The cytotoxicity profiles of these materials were evaluated by protein, MTT, and LDH assays, which demonstrate that all the click clusters remain nontoxic within the expected dosage range while the positive controls, Jet PEI and Superfect, were highly cytotoxic. In particular, **9d** and **9e** were the most effective and promising polycationic vehicles to be further optimized for future systemic delivery experiments.

Introduction

Advancements in medical research are transforming and inspiring the field of supramolecular chemistry.[1−4] Likewise, macromolecular drugs such as siRNA, aptamers, and several oligonucleotide- and gene-based therapies are initiating an exciting paradigm shift in pharmaceutical research.[2−5] Development of novel, selective, and specific nucleic acid drugs for numerous diseases has rapidly increased, and many candidates have high potential to be approved for medicinal use.[6] To realize the tremendous promise of these therapeutics, the central challenge is the design and synthesis of effective, efficient, and selective supramolecular drug delivery vehicles.[4,7,8]

The area of nucleic acid delivery has recently faced a rapid upsurge of interest from researchers in a multitude of fields. Although many creative materials reveal promising biocompatibility and delivery efficiency, the structures are often plagued by being polydisperse in nature, poorly defined, and/or difficult to characterize.[9] Unfortunately, many elegant architectures will not be clinically relevant due to the complex regulatory requirements that must be overcome to obtain approval of new drug candidates for human trials.[3,10] As a result, the development of discrete and well-characterized macromolecules that bind, compact, and deliver nucleic acids in a nontoxic and effective manner remains an immense hurdle in advancing this field toward the clinic.[4,11]

Dendrimers and cluster compounds possess well-defined architectures, precise molecular weights, and multivalent func-

(1) (a) Behr, J.-P. *Acc. Chem. Res.* **1993**, *26*, 274−278. (b) Nielsen, P. E. *Mol. Biotechnol.* **2004**, *26*, 233−248. (c) Wagner, E. *Pharm. Res.* **2004**, *21*, 8−14. (d) Luo, D.; Saltzman, W. M. *Gene Ther.* **2006**, *13*, 585−586. (e) Davis, M. E. *Curr. Opin. Biotechnol.* **2002**, *13*, 128−131. (f) Akhtar, S. *Gene Ther.* **2006**, *13*, 739−740.
(2) Pan, H.; Zheng, Q.; Guo, X. *J. Pept. Sci.* **2007**, *13*, 154−163.
(3) Lee, C. C.; Mackay, J. A.; Frechet, J. M. J.; Szoka, F. C. *Nat. Biotechnol.* **2005**, *23*, 1517−1526.
(4) Boas, U.; Heegaard, P. M. H. *Chem. Soc. Rev.* **2004**, *33*, 43−63.
(5) (a) Anderson, W. F. *Science* **1992**, *256*, 808−813. (b) Katas, H.; Alpar, H. O. *J. Controlled Release* **2006**, *115*, 216−225. (c) Que-Gewirth, N. S.; Sullenger, B. A. *Gene Ther.* **2007**, *14*, 283−291. (d) Rossi, J. J. *Gene Ther.* **2006**, *13*, 583−584. (e) McNamara, J. O., II; Andrechek, E. R.; Wang, Y.; Viles, K. D.; Rempel, R. E.; Gilboa, E.; Sullenger, B. A.; Giangrande, P. H. *Nat. Biotechnol.* **2006**, *24*, 1005−1015. (f) Langer, R.; Tirrell, D. A. *Nature* **2004**, *428*, 487−492.
(6) (a) Boussif, O.; Lezoualc'h, F.; Zanta, M. A.; Mergny, M. D.; Scherman, D.; Demeneix, B.; Behr, J.-P. *Proc. Natl. Acad. Sci. U.S.A* **1995**, *92*, 7297−7301. (b) Meyer, M.; Wagner, E. *Hum. Gene Ther.* **2006**, *17*, 1062−1076. (c) Ooya, T.; Choi, H. S.; Yamashita, A.; Yui, N.; Sugaya, Y.; Kano, A.; Maruyama, A.; Akita, H.; Ito, R.; Kogure, K.; Harashima, H. *J. Am. Chem. Soc.* **2006**, *128*, 3852−3853.
(7) (a) Kim, T.-I.; Baek, J.-U.; Bai, C. Z.; Park, J.-S. *Biomaterials* **2007**, *28*, 2061−2067. (b) Dufès, C.; Uchegbu, I. F.; Schätzlein, A. G. *Adv. Drug Delivery Rev.* **2005**, *57*, 2177−2022. (c) Svenson, S.; Tomalia, D. A. *Adv. Drug Delivery Rev.* **2005**, *57*, 2106−2129.
(8) Tomalia, D. A. *Macromol. Symp.* **1996**, *101*, 243−255.
(9) (a) Breunig, M.; Lungwitz, U.; Liebl, R.; Fontanari, C.; Klar, J.; Kurtz, A.; Blunk, T.; Goepferich, A. *J. Gene Med.* **2005**, *7*, 1287−1298. (b) Hwang, S. J.; Davis, M. E. *Curr. Opin. Mol. Ther.* **2001**, *3*, 183−191. (c) Wightman, L.; Kircheis, R.; Rössler, V.; Carotta, S.; Ruzicka, R.; Kursa, M.; Wagner, E. *J. Gene Med.* **2001**, *3*, 362−372.
(10) Helms, B.; Meijer, E. W. *Science* **2006**, *313*, 929−930.
(11) Duncan, R.; Izzo, L. *Adv. Drug Delivery Rev.* **2005**, *57*, 2215−2237.

10.1021/ja074597v CCC: $40.75

tionalization sites.[12,13] These unique and useful characteristics provide tailorable scaffolds that have motivated their development as nucleic acid carriers. For example, polyamidoamine (PAMAM),[8,14,15] poly-L-lysine dendrimers,[16] dendritic-spermines,[17] -polyesters,[18] and -polypeptides[2,19] have been widely studied for nucleic acid delivery. Higher generations of these structures yield effective delivery.[20] However, chemically functionalizing the large number of peripheral groups on these macromolecules with ligands such as polyethylene glycol (to decrease aggregation and nonspecific interactions), and targeting groups in a well-defined and reproducible manner is complex and sometimes not possible.[15,21] Loss of material definition increases polydispersity of the final delivery vehicle, generates difficulties with structural characterization, and can cause problems in the clinic. Toxicity of these structures has also become a concern that has further hampered development efforts.[11,14,22]

Herein, we describe our approach to achieve a family of discrete macromolecules with versatile features to serve as drug and nucleic acid delivery vehicles. We were inspired by the clinical promise of dendrimers[4,10] and the distinctive features of β-cyclodextrin, which has been shown to serve as a multivalent core in the design of glyco-clusters,[23,24] -conjugates,[25,26] -dendrimers,[27] and star polymers.[28] This cyclic maltooligosaccharide is also endowed with a biocompatible hydrophobic cup-shaped structure that can form inclusion complexes with biologically specific guests. For example, β-cyclodextrin is FDA approved as an adjuvant to aid solubilization of hydrophobic drugs by forming inclusion complexes with the therapeutic molecule, which increases bioavailability.[29] Davis et al. and others have shown that polymers containing β-cyclodextrin units can complex adamantane moieties functionalized with polyethylene glycol (PEG) chains and cell-type specific targeting moieties to discourage nanoparticle flocculation and encourage tissue-specific nucleic acid delivery.[30,31] The present target structures were also motivated by previous work conducted in our group.[32] We have shown that polymers created with alternating saccharide and oligoethyleneamine monomers can effectively complex, condense, and deliver pDNA with exceptional biocompatibility and efficacy.[33,34] Unfortunately, those polymers suffer from polydispersity. The work herein presents the first example of extending this saccharide-oligoamine design motif into a novel family of polycationic β-cyclodextrin click clusters with discrete, monodisperse, and symmetric geometries that reveal promising DNA delivery efficacy without cytotoxicity. This design motif also reveals a prototype of readily tailorable scaffolds with potential to be refined as clinically viable delivery agents for a variety of applications.

In this report, the synthesis of the core moiety, acetylated-per-azido-β-cyclodextrin (**4**), and a novel series of alkyne dendrons (**7a**−**e**) containing between 0 and 4 secondary amines are presented (Schemes 1 and 2). The target macromolecules were assembled employing a convergent approach via the click reaction. This allowed us to avoid subfunctionalized impurities around the sterically hindered core that could elicit unintended biological activity (Scheme 3).[13,35,26] We discovered through gel electrophoresis, dynamic light scattering, and transmission electron microscopy experiments that all the cluster compounds bind and encapsulate pDNA into nanoparticles. These nanoparticles stabilize nucleic acids and protect them from nuclease degradation. In addition, most of the vectors promote high cellular delivery of pDNA (similar to that of Jet-PEI and Superfect, the positive controls) and encourage effective gene

(12) (a) Mulder, A.; Huskens, J.; Reinhoudt, D. N. *Org. Biomol. Chem.* **2004**, *2*, 3409−3424. (b) Smith, D. K. *Chem. Commun.* **2006**, *1*, 34−44. (c) Ihre, H.; Padilla De Jesus, O. L.; Fréchet, J. M. J. *J. Am. Chem. Soc.* **2001**, *123*, 5908−5917.
(13) Hawker, C. J.; Fréchet, J. M. J. *J. Am. Chem. Soc.* **1990**, *112*, 7638−7647.
(14) Braun, C. S.; Vetro, J. A.; Tomalia, D. A.; Koe, G. S.; Koe, J. G.; Middaugh, C. R. *J. Pharm. Sci.* **2005**, *94*, 423−436.
(15) Luo, D.; Haverstick, K.; Belcheva, N.; Han, E.; Saltzman, W. M. *Macromolecules* **2002**, *35*, 3456−3462.
(16) (a) Ohsaki, M.; Okuda, T.; Wada, A.; Hirayama, T.; Niidome, T.; Aoyagi, H. *Bioconjugate Chem.* **2002**, *13*, 510−517. (b) Yamagata, M.; Kawano, T.; Shiba, K.; Mori, T.; Katayama, Y.; Niidome, T. *Bioorg. Med. Chem.* **2007**, *15*, 526−532. (c) Vlasov, G. P.; Korol'kov, V. I.; Pankova, G. A.; Tarasenko, I. I.; Baranov, A. N.; Glazkov, P. B.; Kiselev, A. V.; Ostapenko, O. V.; Lesina, E. A.; Baranov, V. S. *Russ. J. Bioorg. Chem.* **2004**, *30*, 12−20.
(17) (a) Kostiainen, M. A.; Hardy, J. G.; Smith, D. K. *Angew. Chem., Int. Ed.* **2005**, *44*, 2556−2559. (b) Hardy, J. G.; Kostiainen, M. A.; Smith, D. K.; Gabrielson, N. P.; Pack, D. W. *Bioconjugate Chem.* **2006**, *17*, 172−178.
(18) (a) Grinstaff, M. W. *Chem. Eur. J.* **2002**, *8*, 2838−2846. (b) Gvili, K.; Benny, O.; Danino, D.; Machluf, M. *Biopolymers* **2007**, *85*, 379−391. (c) Wu, D.; Liu, Y.; Jiang, X.; He, C.; Goh, S. H.; Leong, K. W. *Biomacromolecules* **2006**, *7*, 1879−1883.
(19) Sadler, K.; Tam, J. P. *Rev. Mol. Biotechnol.* **2002**, *90*, 195−229.
(20) (a) Gillies, E. R.; Fréchet, J. M. J. *Drug Discovery Today* **2005**, *10*, 35−43. (b) Gillies, E. R.; Fréchet, J. M. J. *J. Am. Chem. Soc.* **2002**, *124*, 14137−14146.
(21) (a) Petersen, H.; Fechner, P. M.; Martin, A. L.; Kunath, K.; Stolnik, S.; Roberts, C. J.; Fischer, D.; Davies, M. C.; Kissel, T. *Bioconjugate Chem.* **2002**, *13*, 845−854. (b) Lee, J. H.; Lim, Y.-B.; Choi, J. S.; Lee, Y.; Kim, T.-I.; Kim, H. J.; Yoon, J. K.; Kim, K.; Park, J.-S. *Bioconjugate Chem.* **2003**, *14*, 1214−1221.
(22) (a) Jevprasesphant, R.; Penny, J.; Jalal, R.; Attwood, D.; McKeown, N. B.; D'Emanuele, A. J. *Int. J. Pharm.* **2003**, *252*, 263−266. (b) Malik, N.; Wiwattanapatapee, R.; Klopsch, R.; Lorenz, K.; Frey, H.; Weener, J. W.; Meijer, E. W.; Paulus, W.; Duncan, R. *J. Controlled Release* **2000**, *65*, 133−148.
(23) (a) André, S.; Kaltner, H.; Furuike, T.; Nishimura, S.-I.; Gabius, H.-J. *Bioconjugate Chem.* **2004**, *15*, 87−98. (b) Furuike, T.; Sadamoto, R.; Niikura, K.; Monde, K.; Sakairi, N.; Nishimura, S. -I. *Tetrahedron* **2005**, *61*, 1737−1742. (c) Ortiz-Mellet, C.; Benito, J. M.; García Fernández, J. M.; Law, H.; Chmurski, K.; Defaye, J.; O'Sullivan, M. L.; Caro, H. N. *Chem. Eur. J.* **1998**, *4*, 2523−2531. (d) Fulton, D. A.; Stoddart, J. F. *Org. Lett.* **2000**, *2*, 1113−1116.
(24) Boger, J.; Corcoran, R. J.; Lehn, J.-M. *Helv. Chim. Acta* **1978**, *61*, 2190−2218.
(25) García-López, J. J.; Hernández-Mateo, F.; Isac-García, J.; Kim, J. M.; Roy, R.; Santoyo-González, F.; Vargas-Berenguel, A. *J. Org. Chem.* **1999**, *64*, 522−531.
(26) Pérez-Balderas, F.; Ortega-Muñoz, M.; Morales-Sanfrutos, J.; Hernández-Mateo, F.; Calvo-Flores, F. G.; Calvo-Asyn, J. A.; Isac-García, J.; Santoyo-González, F. *Org. Lett.* **2003**, *5*, 1951−1954.
(27) (a) Ortega-Caballero, F.; Giménez-Martínez, J. J.; García-Fuentes, L.; Ortiz-Salmerón, E.; Santoyo-González, F.; Vargas-Berenguel, A. *J. Org. Chem.* **2001**, *66*, 7786−7795. (b) Jayaraman, N.; Stoddart, J. F. *Tetrahedron Lett.* **1997**, *38*, 6767−6770. (c) Turnbull, W. B.; Stoddart, J. F. *Rev. Mol. Biotechnol.* **2002**, *90*, 231−255. (d) Vargas-Berenguel, A.; Ortega-Caballero, F.; Santoyo-González, F.; García-López, J. J.; Giménez-Martínez, J. J.; García-Fuentes, L.; E, Ortiz.-Salmerón, E. *Chem. Eur. J.* **2002**, *8*, 812−827.
(28) (a) Hoogenboom, R.; Moore, B. C.; Schubert, U. S. *Chem. Comm.* **2006**, *38*, 4010−4012. (b) Yang, C.; Li, H.; Goh, S. H.; Li, J. *Biomaterials* **2007**, *28*, 3245−3254.
(29) (a) Mocanu, G.; Vizitiu, D.; Carpov, A. *J. Bioact. Compat. Pol.* **2001**, *16*, 315−342. (b) Cryan, S.-A.; Holohan, A.; Sonohue, R.; Darcy, R.; O'Driscoll, C. M. *Eur. J. Pharm. Sci.* **2004**, *21*, 625−633.
(30) (a) Hwang, S. J.; Bellocq, N. C.; Davis, M. E. *Bioconjugate Chem.* **2001**, *12*, 280−290. (b) Reineke, T. M.; Davis, M. E. *Bioconjugate Chem.* **2003**, *14*, 247−254.
(31) Bellocq, N. C.; Pun, S. H.; Jensen, G. S.; Davis, M. E. *Bioconjugate Chem.* **2003**, *14*, 1122−1132.
(32) (a) Liu, Y.; Reineke, T. M. *J. Am. Chem. Soc.* **2005**, *127*, 3004−3015. (b) Liu, Y. W. L.; Lynch, M.; Reineke, T. M. In *Polymeric Drug Delivery Volume I - Particulate Drug Carriers*; Svenson, S., Ed.; American Chemical Society: Washington, DC, 2005; Vol. 923, pp 217−227. (c) Srinivasachari, S.; Liu, Y.; Zhang, G.; Prevette, L.; Reineke, T. M. *J. Am. Chem. Soc.* **2006**, *128*, 8176−8184. (d) Prevette, L. E.; Kodger, T. E.; Reineke, T. M.; Lynch, M. E. *Langmuir* **2007**, *23*, 9773−9784.
(33) Liu, Y.; Reineke, T. M. *Bioconjugate Chem.* **2006**, *17*, 101−108.
(34) Liu, Y.; Reineke, T. M. *Bioconjugate Chem.* **2007**, *18*, 19−30.
(35) (a) Calvo-Flores, F. G.; Isac-García, J.; Hernández-Mateo, F.; Pérez-Balderas, F.; Calvo-Asín, J. A.; Sanchéz-Vaquero, E.; Santoyo-González, F. *Org. Lett.* **2000**, *2*, 2499−2502. (b) Yoon, K.; Goyal, P.; Weck, M. *Org. Lett.* **2007**, *9*, 2051−2054. (c) Lee, J. W.; Kim, J. H.; Kim, H. J.; Han, S. C.; Kim, J. H.; Shin, W. S.; Jin, S.-H. *Bioconjugate Chem.* **2007**, *18*, 579−584. (d) Binder, W. H.; Sachsenhofer, R. *Macromol. Rapid Commun.* **2007**, *28*, 15−54.

Scheme 1. Synthesis of Acetylated Perazido-β-cyclodextrin[a]

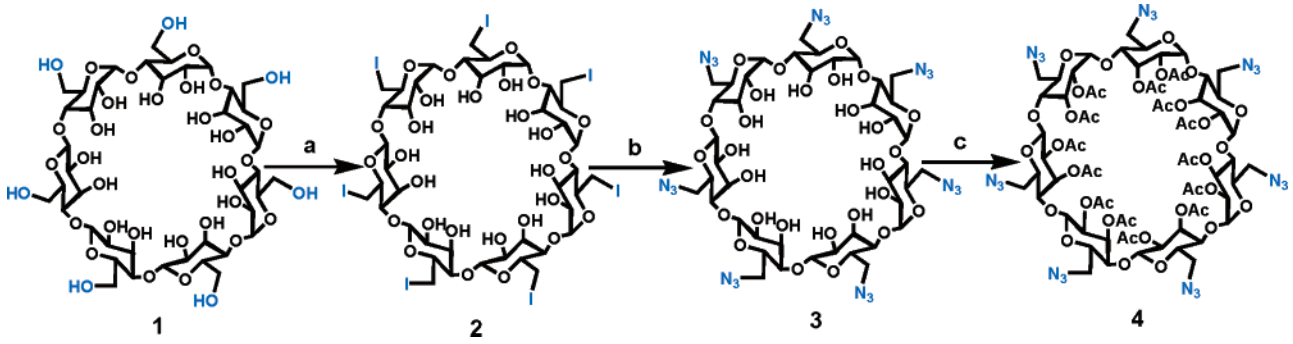

[a] Conditions: (a) PPh_3/I_2, DMF, 80 °C, 18 h; (b) NaN_3, DMF, 80 °C, 24 h; (c) Ac_2O, Pyr, 24 h, RT.

Scheme 2. Synthesis of the Alkyne Dendrons (**7a**−**e**)[a]

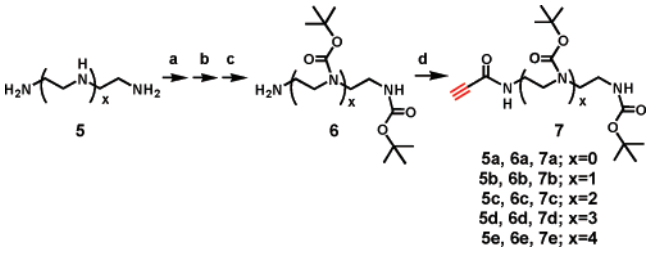

[a] Conditions: (a) CF_3COOEt, MeOH; (b) $(Boc)_2O$, CH_2Cl_2, TEA; (c) K_2CO_3, 20:1, MeOH: H_2O; (d) propiolic acid, DCC, CH_2Cl_2.

Scheme 3. Synthesis of the Click Clusters (**9a**−**e**)[a]

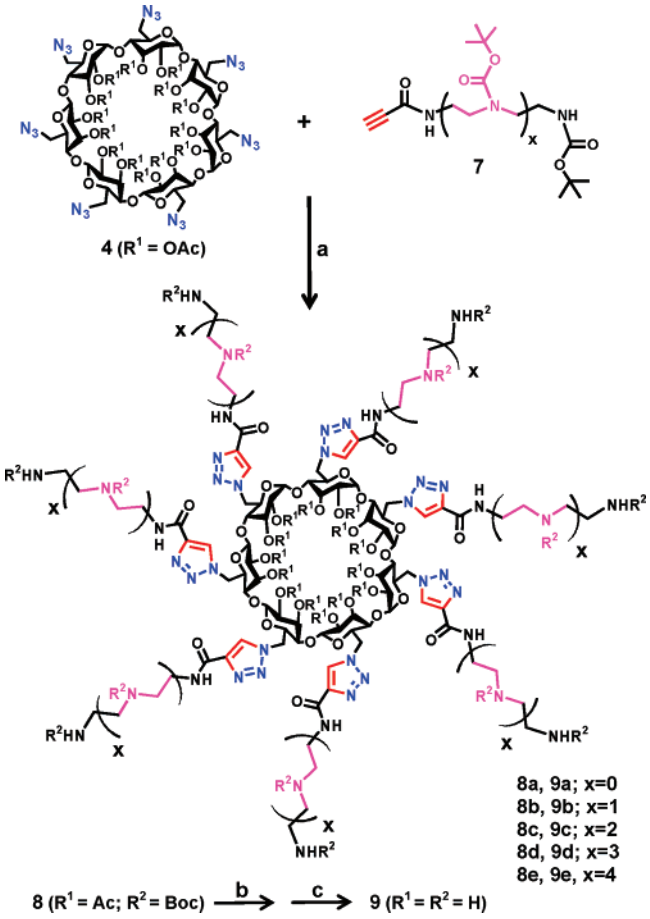

[a] Conditions: (a) $CuSO_4 \cdot 5H_2O$, sodium ascorbate, tBuOH: H_2O (1:1), 70 °C; (b) NaOMe/MeOH, pH = 9, RT; (c) 4 M HCl/dioxane.

expression in both HeLa (human cervix carconima) and H9c2 (rat cardiomyoblast) cell lines. In contrast to the positive controls, these structures reveal low toxicity and do not disrupt cell surface function *in vitro*. The monodisperse macromolecules designed here represent an incredibly unique multivalent architecture that can readily be functionalized via noncovalent (inclusion in the hydrophobic cup) and/or covalent means in a well-defined manner that can be completely characterized via conventional spectroscopic methods. This creative motif represents an important scientific step toward the development of efficient, nontoxic, fully functionalized, and readily tailorable macromolecules with discrete molecular weight for a variety of clinical delivery applications.

Results and Discussion

Synthesis and Characterization of Monomers and Click Clusters. First, the carbohydrate core, acetylated per-azido-β-cyclodextrin (**4**), was synthesized in 72% yield, according to a combination of previously reported methods (Scheme 1).[24,36] Second, we designed a novel series of alkyne dendrons (**7a**−**e**) containing a terminal acetylene group and *tert*-butoxycarbonyl (Boc)-protected secondary amines (five structures that varied in secondary amine stoichiometry, 0−4, Scheme 2). In brief, the dendrons were synthesized by selectively protecting one of the terminal primary amine groups of either diethylenetriamine, triethylenetetramine, tetraethylenepentamine, or pentaethylenehexamine (**5b**−**e**) with a trifluoroacetyl ($COCF_3$) group, followed by *in situ* protection of the remaining terminal primary amine and internal secondary amine(s) with $(Boc)_2O$ to yield the Boc derivatives.[37] The trifluoroacetyl groups were then cleaved to yield the Boc-protected monoamines (**6b**−**e**, Scheme 2), which were coupled to propiolic acid via DCC (dicyclohexylcarbodiimide). Purification of the products via silica gel column chromatography afforded the pure dendrons (**7b**−**e**) in 40−60% yield. Dendron **7a** was synthesized using a similar method, by coupling mono-Boc-protected ethylenediamine (**6a**) with propiolic acid.

The 1,3-dipolar cycloaddition of azide **4** and each alkyne (**7**a−**e**) was carried out using copper sulfate/sodium ascorbate in 1:1 t-BuOH/H_2O to yield the series of protected click clusters (**8**a−**e,** Scheme 3) bearing the regiospecific 1,4-triazole, verified via NMR, in 80% yield.[26,38,39] The products were washed with

(36) Ashton, P. R.; Gattuso, G.; Königer, R.; Stoddart, J. F.; Williams, D. J. *J. Org. Chem.* **1996**, *61*, 9553−9555.
(37) Geall, A. J.; Taylor, R. J.; Earll, M. E.; Eaton, M. A. W.; Blagbrough, I. S. *Bioconjugate Chem.* **2000**, *11*, 314−326.
(38) Rostovtsev, V. V.; Green, L. G.; Fokin, V. V.; Sharpless, K. B. *Angew. Chem., Int. Ed.* **2002**, *41*, 2596−2599.

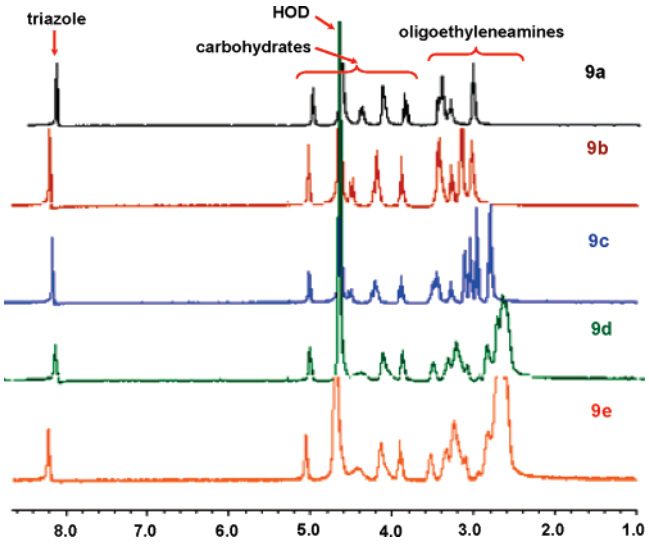

Figure 1. ^{1}H NMR of clusters **9a**−**e** in D_2O (400 MHz).

ammonium hydroxide to remove trace amounts of copper and used without further purification. Conventional deprotection of the acetyl[25] and the Boc[40] groups afforded the final highly water soluble click clusters (**9a**−**e**) in approximately 50% yield. Compounds (**9a**−**c**) were purified via exhaustive dialysis against ultrapure water, whereas compounds (**9d** and **9e**) were purified using cation exchange column with a gradient elution of ammonium bicarbonate and lyophilized to dryness. The final compounds **9a**−**e** were characterized using several techniques to verify complete substitution and pure product formation. The proton peaks were assigned using a combination of ^{1}H NMR and 2D COSY experiments. As shown in Figure 1, the ^{1}H NMR showed the presence of the triazole proton around 8.2 ppm which indicated the formation of the 1,4-regioisomer exclusively.[41] In addition, 2D NOESY (^{1}H−^{1}H) experiments showed strong NOE effects, due to the close proximity of the triazole and N-substituted methylene protons, an effect normally observed in the 1,4-regioisomer.[39] The absence of peaks at 1.4 ppm (Boc) and 2.0 ppm (acetyl) clearly showed the complete deprotection of the acetate and carbamate protecting groups (Figure 1). It should be noted that this step also aids in the full removal of copper from the final materials, as chelated copper may cause unwanted toxicity. The IR spectra also confirmed the absence of azide and alkyne functionalities. The ESI-MS showed peaks corresponding only to the fully substituted materials, as multiply-charged ions (Figure 2). These data support the formation of pure β-cyclodextrin click clusters (**9a**−**e**) decorated through a 1,2,3-triazole linker with a series of dendrons containing both internal secondary amines (between 0 and 4) and terminal primary amines that exhibit a cationic nature at physiological conditions.

Click Cluster−pDNA Binding and Polyplex Size. The final polycations were studied for their ability to bind and compact pDNA into nanoparticles using a variety of methods. Prior to all studies, each cluster was mixed with pDNA at various *N*/*P* ratios (where *N* = primary and secondary amines in the click clusters; *P* = phosphate groups in the pDNA) in DNase/RNase-free water to form the nanoparticle complexes. To confirm complexation, a gel electrophoresis shift assay was first performed. Figure 3a shows that compound **9e** bound pDNA at *N*/*P* ratios of 1.5 and higher (pDNA lacks migration in the gel due to polycation binding and charge-neutralization). The bars in Figure 3c reveal that all of the click clusters fully complex pDNA between *N*/*P* ratios of 1.5 and 2.5, dependent on the length of the dendron arm. To assess and compare the relative binding stability, a heparin competitive displacement assay was performed on the nanoparticles formed with **9a**−**e** and pDNA at a complexation ratio of *N*/*P* = 5. As pictured in Figure 3b, complexes formed with **9e** and pDNA required a concentration of 110 μg/mL of heparin to dissociate the binding (shown by the migration of pDNA in the gel). The binding affinities of the clusters for pDNA measured via gel shift assay were corroborated with the heparin displacement results (line, Figure 3c), where the relative binding stability (heparin concentration that dissociated the polyplexes) was found to be **9a** (200 μg/mL) > **9e** (110 μg/mL) > **9d** (100 μg/mL) > **9c** (90 μg/mL) > **9b** (80 μg/mL). In general, nanoparticle stability improved with increase in cluster arm length. This could be due to an enhancement in electrostatic and H-bonding interac-

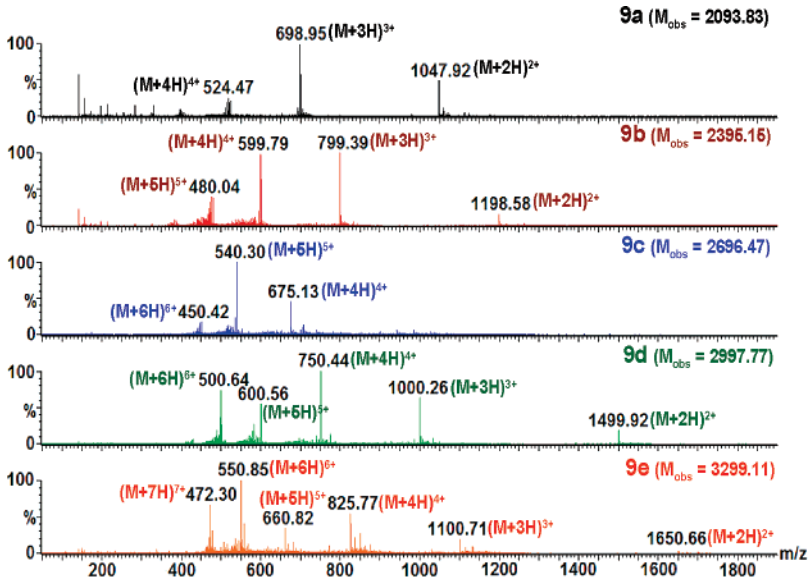

Figure 2. ESI-MS of clusters **9a**−**e**. The labeled masses are for the observed monoisotopic ions. The M_{obs} is a deconvoluted mass of the compounds from multiply charged ions.

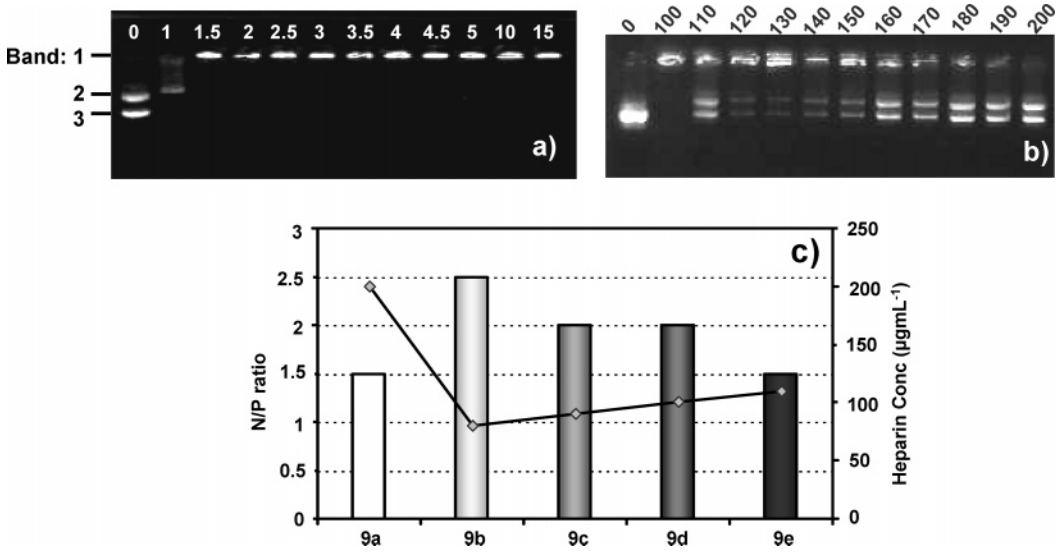

Figure 3. Agarose gel electrophoresis pDNA−click cluster binding assays. (a) Gel shift assay showing **9e**−pDNA binding at *N*/*P* ratios between 0 (pDNA only) and 15. Binding is shown by the inhibition of pDNA electrophoretic mobility (band 1). Bands 2 and 3 show the relaxed and supercoiled forms of pDNA respectively. (b) The concentration of heparin (μgmL^{-1}) required to release pDNA from click cluster−**9e** binding (polyplexes formed at $N/P = 5$). Heparin dissociation from **9e** is shown by the appearance of pDNA electrophoretic mobility. (c) The minimum *N*/*P* ratio needed to inhibit electrophoretic mobility in the click cluster gel shift assays (bars) and the relative binding affinity of each click cluster−pDNA complex as determined by the concentration of heparin required to release pDNA from each complex (line) at $N/P = 5$.

tions as the length of the cluster arms increase (only partial amine protonation is expected with these clusters, titration studies are in progress).[34,42] We were surprised by the unusually high heparin concentration needed to dissociate compound **9a**, as it did not follow the general trend, and this result could also be related to the cluster size. Cluster **9a** is the smallest in size and may partially bind in the pDNA major groove. Therefore, this complex could be less accessible to competitive displacement by heparin (a large polyanion); if this is the case, smaller anions could promote more effective displacement (*vide infra*).

The compaction of the pDNA into stable nanoparticles in the size range to be endocytosed (50−500 nm) is an important process that impacts cellular uptake. Dynamic light scattering (DLS) and ζ potential experiments were conducted to examine the size and surface charge of the nanoparticles formed at an *N*/*P* ratio of 5. The clusters formed nanoparticles with pDNA having an average hydrodynamic diameter between 80−130 nm (Figure 4) that exhibited near neutral to cationic ζ potentials. In general, the ζ potential experiments revealed an increase in positive polyplex potential as the cluster arm length increased. TEM experiments supported these data, where discrete nanoparticles were observed and imaged (Figure 5).

DNase Protection Assay. The ability of **9a**−**e** to protect pDNA against nuclease degradation (present in FBS, fetal bovine serum) was then examined via gel electrophoresis to verify stable pDNA encapsulation. Nanoparticles were incubated with FBS at 37 °C for 0, 1, 2, 4, or 8 h. Afterwards, SDS was added to dissociate the complexes. The ability of each cluster to protect pDNA from nuclease degradation was determined by examination of pDNA integrity using electrophoresis. As shown in Figure 6, the degraded pDNA was visualized by the appearance of band 6 (degraded small pieces of DNA) and a

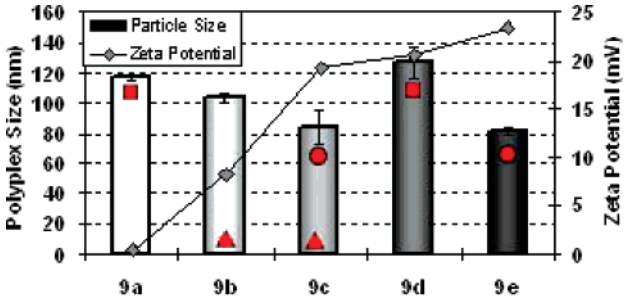

Figure 4. The hydrodynamic diameter of the polycation−pDNA complexes at $N/P = 5$ in nuclease free water as determined via dynamic light scattering (bars) and the ζ-potential of the polyplexes (line). All particle size measurements were found to be statistically different from each other ($p < 0.05$) except for those indicated with similar geometric red symbols.

decrease in intensity of bands 2−4 (nicked, relaxed, and supercoiled pDNA, respectively). It should be noted that band 5 arises from a complex formed between FBS and SDS. Degredation of naked pDNA began immediately upon addition of FBS, as observed by the decrease in the intensity of bands 2−4, and was fully degraded in only 1 h. Plasmid DNA complexed with **9b** began to degrade after 4 h of incubation with FBS (shown by the presence of band 6 and the decrease in intensity of bands 2−4), which is consistent with the gel shift and heparin displacement assays. This indicates that **9b** is the least effective at binding and protecting pDNA against nuclease degradation. A slight decrease in intensity of pDNA bands was observed after incubation of **9a** with FBS for 8 h, possibly indicating some pDNA degradation at this time point and incomplete pDNA encapsulation. Plasmid DNA complexed with click clusters **9c**, **9d**, and **9e** was protected from degradation even after 48 h of exposure to FBS, as shown in Figure 7. These data indicate that the increased amine stoichiometry within the dendrons increases pDNA protection from nuclease degradation and enhances stable encapsulation.

Salt-Induced Polyplex Dissociation. It is important to understand the unpackaging properties of the click clusters, since

(39) Tornøe, C. W.; Christensen, C.; Meldal, M. *J. Org. Chem.* **2002**, *67*, 3057−3064.
(40) Han, G.; Tamaki, M.; Hruby, V. J. *J. Pept. Res.* **2001**, *58*, 338−341.
(41) Fazio, F.; Bryan, M. C.; Blixt, O.; Paulson, J. C.; Wong, C.-H. *J. Am. Chem. Soc.* **2002**, *124*, 14397−14402.
(42) Suh, J.; Paik, H.-J.; Hwang, B. K. *Bioorg. Chem.* **1994**, *22*, 318−327.

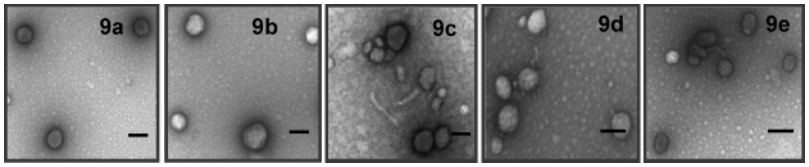

Figure 5. Transmission electron micrograph of the nanoparticles formed with **9a**−**e** and pDNA at $N/P = 5$ in water. Nanoparticles were visualized via negative staining with uranyl acetate, where the bar represents 100 nm.

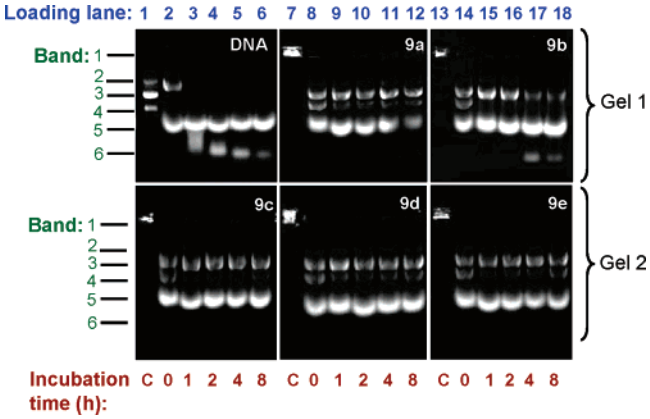

Figure 6. Protection of pDNA from nuclease degradation (present in FBS) by **9a** (lanes 7−12; gel 1), **9b** (lanes 13−18; gel 1), **9c** (lanes 1−6; gel 2), **9d** (lanes 7−12; gel 2), and **9e** (lanes 13−18; gel 2) complexed at $N/P = 5$. Naked pDNA (lanes 1−6; gel 1) was used as a control. Other control samples analyzed were (labeled as C for the incubation time): pDNA only (lane 1, gel 1) and complexes formed with pDNA and **9a** (lane 7, gel 1), **9b** (lane 13, gel 1), **9c** (lane 1, gel 2), **9d** (lane 7, gel 2), and **9e** (lane 13, gel 2) without addition of FBS and SDS. Band 1 is the position of the sample loading (polyplexes without FBS and SDS treatment). Bands 2−4 are nicked, relaxed, and supercoiled pDNA, respectively. Band 5 results from a complex of FBS and SDS, and band 6 is degraded DNA.

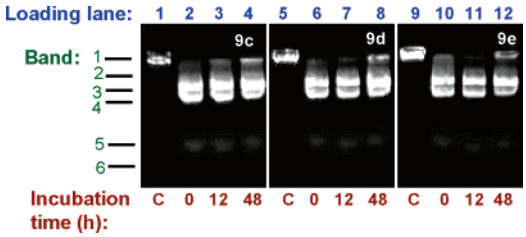

Figure 7. Protection of pDNA from nuclease degradation (present in FBS) by **9c** (lanes 1−4), **9d** (lanes 4−8), and **9e** (lanes 9−12) complexed at $N/P = 5$. Band 1 is the position of the sample loading (polyplexes without FBS and SDS treatment). Bands 2−4 are nicked, relaxed, and supercoiled pDNA, respectively. Band 5 results from a complex of FBS and SDS, and band 6 is degraded DNA.

release of therapeutic DNA after its delivery is a crucial process in transfection. The dissociation of pDNA from the clusters was studied via PicoGreen, a fluorescent intercalating DNA dye, as a function of NaCl concentration.[43] It is known that increased salt concentrations can destabilize the binding between nonviral vectors and DNA by decreasing their electrostatic interaction, thus leading to decomplexation and/or pDNA release. This allows increased PicoGreen intercalation, thus resulting in an enhanced fluorescence. As shown in Figure 8, the PicoGreen did not intercalate into pDNA molecules complexed by polycations **9a**, **9b**, **9c**, **9d**, and **9e**, resulting in almost 100% PicoGreen exclusion, without NaCl addition. However, after the addition of various concentrations of NaCl (0.1−0.7 M), we observed an increase in fluorescence due to increased Picogreen

(43) Akinc, A.; Thomas, M.; Klibanov, A. M.; Langer, R. *J. Gene. Med.* **2005**, *7*, 657−663.

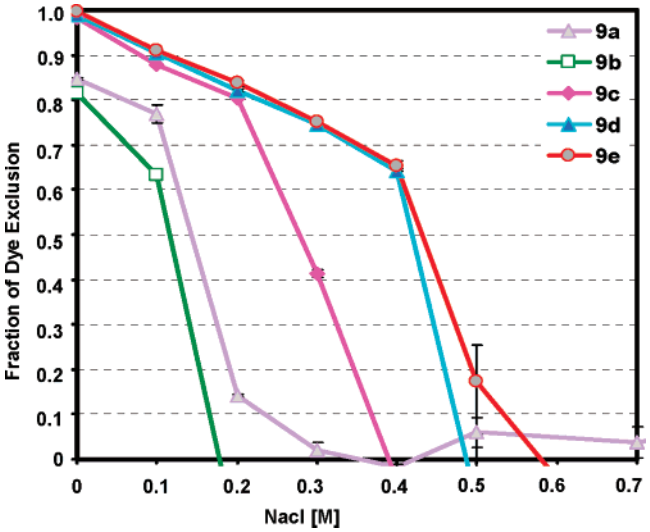

Figure 8. Polyplex dissociation with $NaCl_{(aq)}$. The fraction of dye exclusion [1 − fraction of PicoGreen intercalation (normalized to PicoGreen intercalation of naked pDNA)] when polyplexes formed with **9a**, **9b**, **9c**, **9d**, or **9e** are exposed to increasing concentrations of NaCl.

intercalation into pDNA upon vector release. The concentrations of NaCl that allowed 50% dye inclusion for click clusters **9a**, **9b**, **9c**, **9d**, and **9e** were roughly 0.160 M, 0.125 M, 0.280, 0.425, and 0.440 M, respectively, which represented a qualitative order of binding strength: **9b** < **9a** < **9c** < **9d** < **9e**. Therefore, this study further corroborates the correlation between pDNA binding and cluster arm length (amine stoichiometry) previously supported by gel shift, heparin displacement, and nuclease degradation experiments. In general, as the oligoethyleneamine length decreased, the pDNA was unpackaged at lower NaCl concentrations, indicating a weaker binding affinity. Cluster **9b** was found to have the lowest binding strength (unpackaged pDNA the easiest), which correlates directly to the gel shift assay, heparin competitive displacements, and nuclease degradation results that shorter dendrons decrease encapsulation stability. However, cluster **9a** was found to have a binding affinity similar to (only slightly higher than) **9b**, which did not correlate to the heparin experiments. This experiment supports our hypothesis that the smallest click cluster, **9a**, may partially bind in the pDNA major groove and could be masked from displacement with a large polyanion such as heparin. Here, **9a** was found to be readily displaced at relatively low concentrations with a smaller anion (Cl^-), which correlates directly to the nuclease degradation experiments.

Cellular Delivery and Toxicity Studies. The delivery of nucleic acids into cells with synthetic materials involves a complex route that requires the nanoparticles to circumvent many destructive obstacles during cellular delivery. Subsequently, the ability of each click cluster to deliver pDNA into mammalian cells was screened via flow cytometry experiments in the HeLa (human cervix adenocarcinoma) and H9c2 (rat

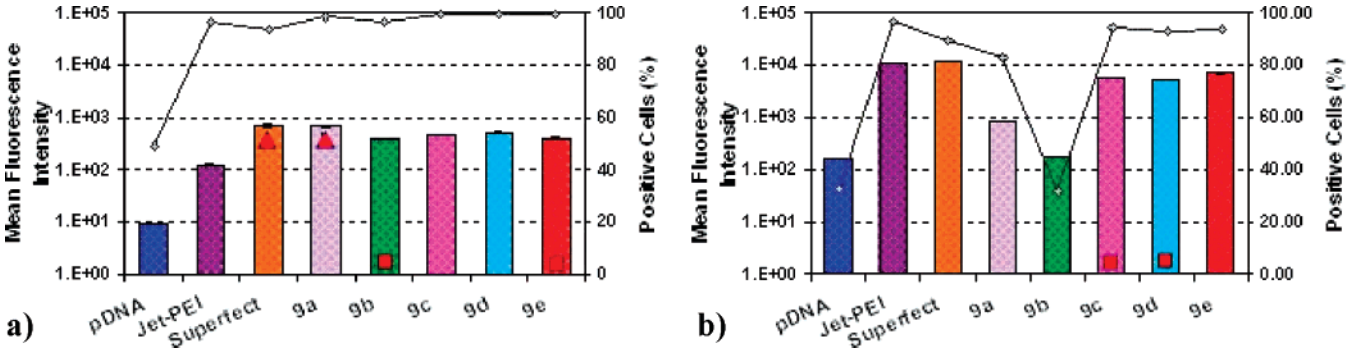

Figure 9. Flow cytometry analysis of pDNA delivery with **9a**−**e** ($N/P = 20$) and the controls, DNA only, Jet-PEI ($N/P = 5$), and Superfect ($N/P = 5$). Both charts depict the mean fluorescence intensity (bars) and the percentage of cells positive for Cy5 fluorescence (lines) in Opti-MEM conditions for (a) HeLa cells and (b) H9c2 cells. Each data point represents the mean ± standard deviation of three replicates. All Cy5 fluorescence intensity measurements were found to be statistically different from each other ($p < 0.05$) except for those indicated with similar geometric red symbols.

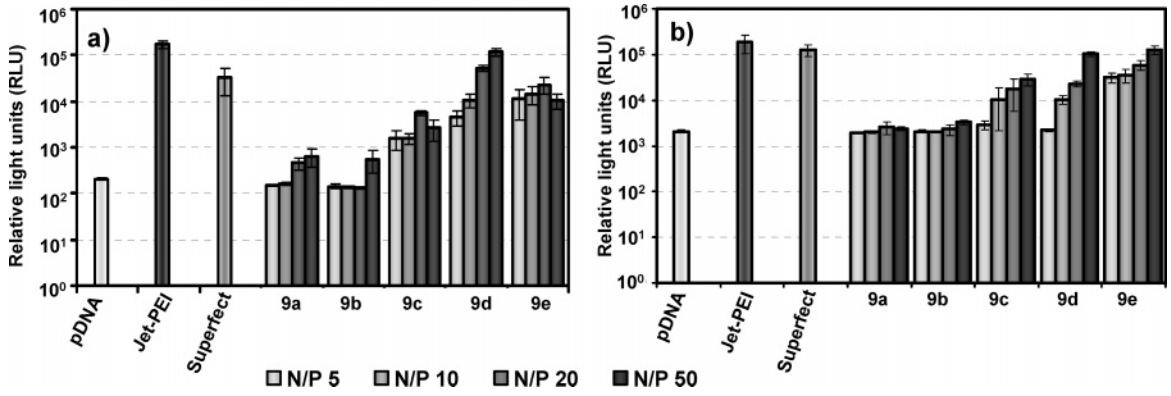

Figure 10. Luciferase gene expression with HeLa and H9c2 cells transfected with each cluster in Opti-MEM. Complexes were formed at N/P ratios of 5, 10, 20, and 50, with each vector (**9a**−**e**) and pDNA. The N/P ratio that exhibits the maximum gene expression of the positive controls, Jet-PEI and Superfect, is 5. (a) Transfection efficiency of vectors in HeLa cells. (b) Transfection efficiency of vectors in H9c2 cells. Each data point represents the mean ± standard deviation of three replicates. Statistical significance of the data is available in the Supporting Information.

cardiomyoblast) cell lines, in the presence of Opti-MEM (serum-free media). Jet-PEI and Superfect were used as positive controls (at $N/P = 5$, which is the recommended concentration for most effective delivery). The flow cytometry experiments were performed at $N/P = 20$, to quantify the cellular uptake of Cy5-labeled pDNA complexed with **9a**−**e**, and the results are shown in Figure 9. This N/P ratio was chosen as it represented high efficacy with low toxicity as determined by gene expression and toxicity assays (*vide infra*). The charts depict the percentage of cells positive for Cy5-labeled pDNA (lines) and the relative amount of Cy5-pDNA delivered per cell, displayed as the mean fluorescence intensity (bars) for HeLa Cells (Figure 9a) and H9c2 cells (Figure 9b). These data indicate that all of the click clusters are very effective at promoting cellular uptake of pDNA *in vitro* to HeLa cells. In the HeLa cells, greater than 95% of cells treated with click cluster−pDNA complexes were positive for Cy5-labeled pDNA when transfected in Opti-MEM, which was similar to the positive controls Jet-PEI and Superfect. However, it should be noted that two cell populations were observed in the flow cytometry data obtained with Superfect, which is likely a result of its extreme toxicity in Opti-MEM (*vide infra*). In addition, when comparing the relative mean pDNA fluorescence intensity (amount of pDNA per cell), the clusters were about as effective as Superfect; however, Jet-PEI revealed an order of magnitude lower fluorescence intensity, indicating that this vector does not carry as much pDNA into cells as the cluster-based vehicles. In the H9c2 cell line, cellular uptake of Jet-PEI and Superfect were similar both in the mean Cy5 fluorescence intensity of cells and percent of cells positive for Cy5 fluorescence. However, **9a** and **9b** had significantly lower cellular uptake then the rest of the vectors. The difference noticed in the cellular uptake when comparing the HeLa and H9c2 data may be a result of the difference in the nature between the cell surfaces. It has previously been demonstrated that the expression patterns of heparan sulfate proteoglycans varies drastically in different cell types, with HeLa cells demonstrating very high expression.[44] This increase in anionic proteoglycan surface environment could permit increased uptake of **9a** and **9b** in HeLa cells in comparison with H9c2 cells. With H9c2 cells, only vectors **9c**−**e** show high cellular uptake, similar to that of the positive controls. Altogether, the uptake data for both cell lines indicated that the click clusters with the longest oligoethyleneamine arms are most effective at delivering pDNA into differing cell types in Opti-MEM.

The transfection efficiency of the click clusters were also studied by performing luciferase reporter gene expression experiments with HeLa and H9c2 cells at a variety of N/P ratios (5, 10, 20, and 50), in Opti-MEM. Jet-PEI and Superfect were again used as positive controls. The luciferase gene expression profiles for both cell lines, shown in Figure 10, indicate that the delivery efficiency generally increased with the N/P ratio for clusters **9a**−**e**. With HeLa cells, **9d** had the highest transfection efficiency of all the click clusters, whereas **9a** and **9b** showed only moderate efficacy even at high N/P ratios. It

(44) Pajusola, K.; Gruchala, M.; Joch, H.; Lüscher, T. F.; Ylä-Herttuala, S. *J. Virol.* **2002**, *76*, 11530−11540.

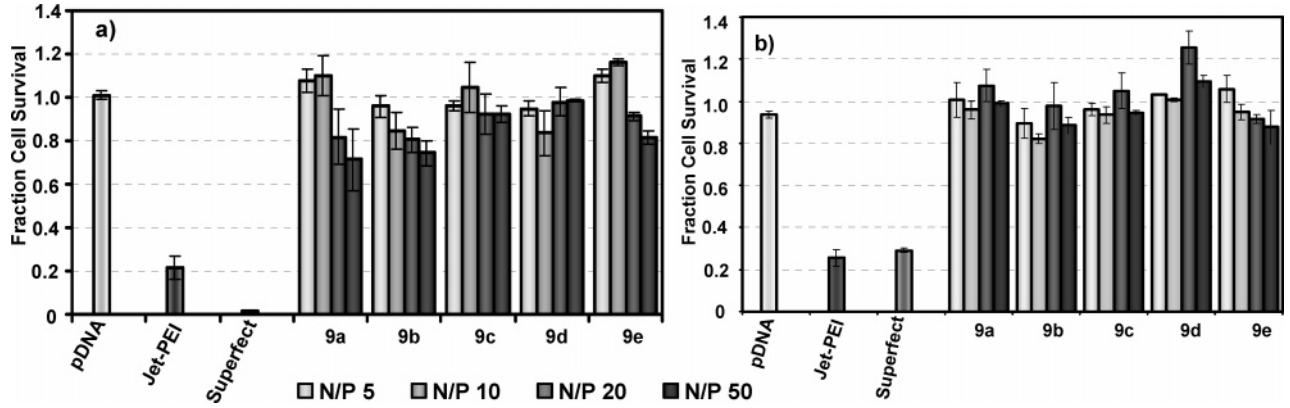

Figure 11. Cell viability of (a) HeLa cells and (b) H9c2 cells 48 h after polyplex exposure as measured by protein content. Polyplexes were formed with **9a**−**e** and pDNA at *N*/*P* of 5, 10, 20, and 50, and incubated in Opti-MEM. The polyplexes were formulated Jet-PEI and Superfect and *N*/*P* = 5. Each data point represents the mean ± standard deviation of three replicates. Statistical significance of the data is available in the Supporting Information.

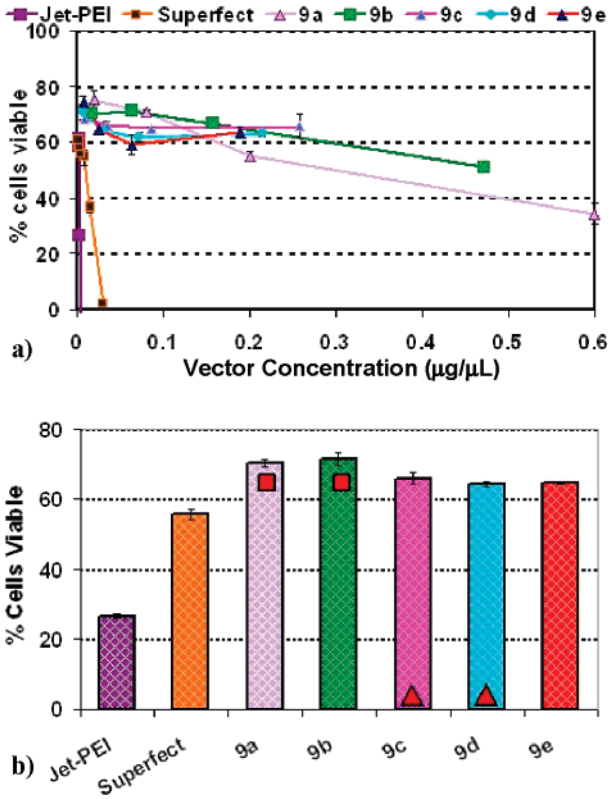

Figure 12. (a) MTT assay of **9a**−**e** in HeLa cells after 32 h of exposure to vector. Cells were treated with the click clusters at four different concentrations correlating to the *N*/*P* ratios of 150, 50, 20, and 5 used in transfection studies. Jet-PEI and Superfect vectors were administered to cells at six concentrations similar to those used to formulate polyplexes at *N*/*P* = 5. Each data point represents the mean ± standard deviation of three separate measurements. (b) Statistical analysis of the cell viability of HeLa cells measured via MTT assay. Bars indicate the percentage of cells viable (at *N*/*P* 5 for Jet-PEI and Superfect; at *N*/*P* 20 for the click clusters). All measurements were found to be statistically different from each other ($p < 0.05$) except for those indicated with similar geometric red symbols.

was not a surprise to find that **9b** displayed the lowest gene expression, which was consistent with the previous data and likely due to the weak binding affinity and lack of pDNA protection against enzymatic degradation. Transfection in the H9c2 cell line supports that **9d** and **9e** are most efficacious click clusters. Although the trends differ slightly between cell lines, differences in growth rate and intracellular trafficking mechanisms may be the cause for the observed differences. However, transfections of both cell lines revealed that **9d** and **9e** are similarly as efficient as the positive controls. The high efficacy of these two click clusters is likely due to a combination of features. Vectors **9d** and **9e** deliver pDNA into 95−100% of HeLa and H9C2 cells, and these two vectors exhibit high stability from salt and heparin-induced unpackaging. Also, **9d** and **9e** prohibited pDNA denegration, and therefore likely promotes a higher delivery rate of expression-competent pDNA during the transfection process. It should be noted that when the data were normalized to the milligrams of protein, Jet-PEI appears artificially high due to the high toxicity (very low amount of protein present) (see Supporting Information). With HeLa cells, Superfect was highly toxic and the protein content was virtually undetectable (thus transfection efficiency was unable to be normalized to milligrams of protein; see Supporting Information).

The cell viability profiles were first measured via protein content in both the HeLa and H9c2 cell lines after transfection in Opti-MEM (Figure 11). The results demonstrate that the click clusters have minimal cytotoxic effects to cultured cells (viability at or above 75%) even at an *N*/*P* of 50. Jet-PEI and Superfect were found to exhibit high toxicity with both cell lines when compared to click clusters. It should be noted here that Jet-PEI is a polydisperse material and Superfect is a fractured dendrimer. Therefore, in addition to the toxicity, the synthesis of identical batches of Jet-PEI and Superfect could be an issue at a clinical scale. The above promising results show that these discrete monodisperse cyclodextrin-based click clusters have high biocompatibility and efficacy *in vitro* and warrant investigation for *in vivo* nucleic acid delivery, which is planned in our future studies.

An MTT assay was performed on HeLa and H9c2 cells treated with the click clusters (not polyplex) to get a more accurate assessment of the cytotoxicity (Figure 12). This assay relies on the rate of a crucial mitochondrial enzyme as a measure of cell survival. In this assay, the results correlate with the protein assay (Figure 11). Clusters **9a** and **9b** appear to decrease cell viability at very high vector concentrations. This experiment further demonstrates the toxicity of the positive controls, revealing that concentrations less than 0.1 μg/mL cause complete cell death. The positive controls, Superfect and Jet-PEI, exhibited an LD_{50} value of 0.0073 μg/uL and 0.0010 μg/uL, respectively. These concentrations are much less than those used when formulating polyplexes at an *N*/*P* ratio of 5. An LD_{50} value

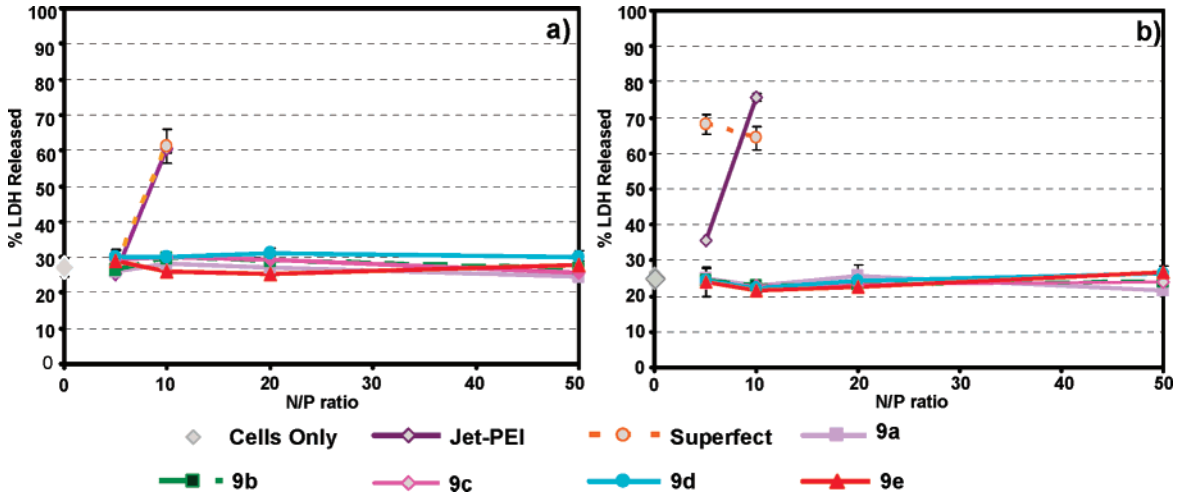

Figure 13. Membrane integrity of HeLa cells reported as the percentage of lactate dehydrogenase (LDH) release 5 h after exposure to (a) polyplexes formed with Jet-PEI, Superfect, **9a**, **9b**, **9c**, **9d**, or **9e** and (b) Jet-PEI, Superfect, **9a**, **9b**, **9c**, **9d**, or **9e** only (no pDNA). An LDH assay kit was used to measure the amount of LDH enzyme leakage into the culture the media. A control of lysed cells was used to determine the total amount of LDH present in each sample and normalize to 100% LDH released. Each data point represents the mean ± standard deviation of three separate measurements.

could only be calculated for two clusters, **9a** (0.3525 μg/uL) and **9b** (0.5073 μg/uL). Both of these concentrations are higher than the concentrations needed to form polyplexes at an *N*/*P* ratio of 50. The toxicity of the other click clusters was not high enough to measure LD_{50} values in the concentration range of this experiment. The MTT assays with H9c2 cells showed very similar results (data not shown).

In order to further investigate the biological impact of these polycationic click clusters on cells, an LDH (lactate dehydrogenase) assay was used to measure the membrane integrity of cells treated both with vector alone and with cluster-pDNA nanoparticles. It has previously been demonstrated that very charge dense cations such as PEI and Superfect can damage the plasma membrane of cells, which contributes to the cytotoxicity of these vectors.[45] Furthermore, we wanted to investigate the effect of the β-cyclodextrin-based macromolecules on membrane integrity. It is well-known that a cyclodextrin cup can complex cholesterol and other biological molecules (present on the cell surface); that this may lead to membrane damage and subsequent leakage of LDH from the cytosol. This assay measures the amount of LDH released into the media and uses it as an indication of cell membrane disruption. Controls of lysed cells were used to determine the total amount of LDH present in each sample. This value was used to normalize the experimental samples and determine the total amount of LDH released from these cells (Figure 13). When cells were treated with polyplexes (Figure 13a), it was found that Jet-PEI and Superfect polyplexes do not damage the cell membrane at low *N*/*P* ratios. However, when the polyplex *N*/*P* ratios were increased, significant amounts of LDH were found in the sample media indicating that these vectors induced membrane damage. When this assay was performed with polyplexes formed with the click clusters, full membrane integrity was observed at all *N*/*P* ratios. When cells were treated with the vectors alone (at the respective concentration used to formulate the polyplexes show in Figure 13a), Superfect was found to release 65−70% of cytosolic LDH (Figure 13b), indicating that this vector is very damaging to the cell membrane. Increasing the amount of Superfect does not appear to further increase damage. Conversely, Jet-PEI alone exhibits some membrane damage at low *N*/*P* ratios, but the amount of LDH released increases drastically with the vector dosage, where nearly 80% of LDH release was found. Conversly, the click clusters did not exhibit any evidence of membrane damage, even when cells were treated with vector concentrations much higher than Jet-PEI and Superfect. Therefore, the β-cyclodextrin cups present in the click clusters are not capable of inducing membrane damage. However, increased cell surface binding via β-cyclodextrin inclusion of cell surface groups may increase cellular uptake. This hypothesis is supported by cellular uptake data (Figure 9a) which demonstrates that even vectors with short oligoethyleneamine arms (**9a**, **9b**) elicit high cellular uptake of pDNA.

Conclusion

In summary, a novel series of polycationic β-cyclodextrin "click clusters" have been synthesized by linking a per-azido-β-cyclodextrin core moiety to oligoethyleneamine dendrons via click coupling chemistry. The final clusters, **9a**−**e**, were found to be completely substituted and deprotected according to a variety of characterization techniques. These discrete macromolecules are highly water soluble, and most of the click clusters were found to complex and protect pDNA in a stable manner with size and morphologies similar to viral delivery vehicles. Cellular delivery and viability experiments demonstrate that all of these structures have the ability to deliver Cy5-labeled pDNA and pDNA encoding the luciferase reporter gene into HeLa and H9c2 cells very effectively in Opti-MEM, with low cytotoxic effects. In particular, **9d** and **9e**, with the longest dentron arms, were the most effective delivery vehicles.

The synthetic design and application of these well-defined and characterized structures is very significant and relevant to the development of clinically viable drug delivery vehicles. For example, the terminal primary amines can be symmetrically functionalized with various biologically active groups (such as drug molecules or imaging agents). The hydrophobic cup can

(45) Moghimi, S. M.; Symonds, P.; Murray, J. C.; Hunter, A. C.; Debska, G.; Szewczyk, A. *Mol. Ther* **2005**, *11*, 990−995.

be exploited to host adamantane groups substituted with poly(ethylene glycol) chains to increase stability from aggregation, circulation lifetime, and/or tissue-specific targeting of the nanoparticles for enhanced therapeutic selectivity and specificity.[31] Future experiments are aimed at exploring these unique macromolecules for a variety of biomedical applications.

Acknowledgment. The authors gratefully acknowledge Dr. Larry Sallans (Mass Spec Facility, Dept. of Chemistry, University of Cincinnati) for his immense help in the ESI-MS analyses of the compounds reported in this paper. This work was supported by the NSF CAREER (CHE-0449774) and the Beckman Young Investigators Programs.

Supporting Information Available: Experimental details of the synthesis and characterization of compounds **4**, **7a** −**e**, and **9a** −**e** and details of the electrophoresis, ethidium bromide exclusion assays, TEM, dynamic light scattering, cell culture, flow cytometry, reporter gene, and viability assays. This material is available free of charge via the Internet at http://pubs.acs.org.

JA074597V